Conference Proceedings

Solar World Congress 2015
Daegu, Korea, 08 – 12 November 2015

# STUDY OF A THERMAL–PHOTOVOLTAIC SOLAR HYBRID SYSTEM

**Haruhiko MIYANABE [1], and Keizo YOKOYAMA [1]**

1 Kogakuin University, Japan

### Abstract

The solar hybrid panel used in this research includes, besides a PV part, a heat acquisition part consisting of flat heat pipes and heat collection pipe on the back of the solar PV module. The system is capable of simultaneously converting solar energy into both electricity and heat. It has the potential to improve total solar energy conversion efficiency while reducing generation losses caused by rising temperature of the solar PV module. This study aims to achieve practical use of this solar hybrid panel. The report describes basic characteristic of the heat pipe used for the heat-collecting module. The energy balance of the system was simulated and compared against measurement data. Sensitivity analysis was also performed. As a result, the heat pipe was found to function normally when the angle of tilt is at least 10 degrees.

Keywords: *Photovoltaic, Solar thermal, Hybrid, Experiment, Simulation*

## 1. Introduction

Photovoltaics have become popular throughout the world. Their conversion efficiency is about 10–15%. The current efficiency is not very high. Utilization of solar heat, on the other hand, has a conversion efficiency of 40–50%. However applications of solar heat are limited. Therefore, various studies are being conducted to extend utilization technology (E. Yandri, 2011).

A thermal-solar hybrid system has characteristics of both photovoltaic power generation and solar heat collection. This report provides an overview of demonstration experiments on such a system, and the system's performance characteristics.

## 2. Composition of the thermal-solar hybrid panel

The solar hybrid panel used in this research includes, besides a PV part, a heat acquisition part consisting of flat heat pipes and heat collection pipe on the back of the solar PV module. The system is capable of simultaneously converting solar energy into both electricity and heat (see Fig. 1 and Fig. 2). It has the potential to improve total solar energy conversion efficiency while reducing generation losses caused by rising temperature of the solar PV module. Fig. 3 shows the installed condition and Fig. 4 shows a schematic diagram of the system.

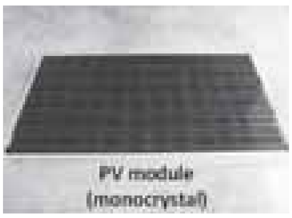


**Fig. 1: Solar hybrid panel**


**Fig. 2: Constitution of the Solar hybrid panel**

**Fig. 3: Appearance of solar hybrid system**

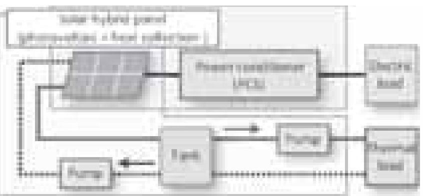

**Fig. 4: Schematic of solar hybrid system**


doi:10.18086/swc.2015.10.04 Available at http://proceedings.ises.org

## 3. Overview of research

Although the aim of this research is to achieve practical use to the solar hybrid panel, this report develops an understanding of the basic characteristics of the heat pipe used in the heat-collecting module. A simple simulation of the energy balance was conducted. Sensitivity analysis was also performed while varying a number of parameters.

## 4. Overview of micro flat heat pipe

Table 1 provides an overview of the heat-collecting module used in the solar hybrid panel. Fig. 3 shows a schematic diagram of heat transfer in the micro flat heat pipe.

The heat pipe has a capillary structure and has a working fluid sealed inside. The principle of heat transfer is as follows: When the heat pipe is heated, working fluid is vaporized, and it moves upward from the bottom of the heat pipe. At the top of the heat pipe, it is condensed by cooling, and when it becomes a liquid it returns again to the bottom of the pipe due to the capillary phenomenon. In this way, heat transfer is carried out continuously.

**Table 1: Overview of heat pipe**

| | |
|---|---|
| Outer dimensions (height x width x thickness) [mm] | 765×60×3 |
| Material | Pure aluminum (extruded) |
| Working fluid | Acetone |
| Thermal conductivity [W/cm$^2$] | 37.35 |
| Isothermality | Less than 1 [K/m] |
| Max. heat flow density [W/cm$^2$] | 100 to 200 |
| Working temperature range [ºC] | -50 to 170 |
| Internal withstand pressure [MPa] | 5.07 or higher |
| External withstand pressure [MPa] | 3.92 |

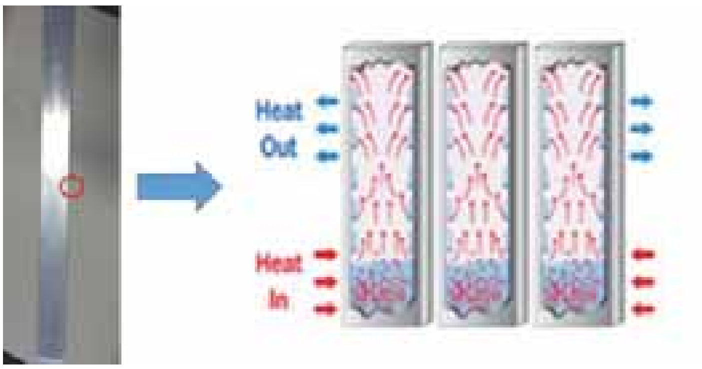


**Fig. 5: Schematic diagram of heat transfer of heat pipe**

## 5. Heat pipe characteristic test

Experiments were conducted to determine how heat transport conditions of the heat pipe changed due to angle of tilt, heat input, presence or lack of insulation on the back side, and differences in length.

### *5.1 Overview of experiment*

The experiment used a mask-formed flat heating element to evenly heat the entire pipe. In a product, the added heat is collected by water at one end of the heat pipe, but in this experiment the heat is radiated to the outside via the air. Figure 3 is a schematic diagram of the solar hybrid panel, and the experimental equipment was built to simulate this, as shown in Fig. 4. Insulation (1 and 2) on the heating element side was used to reduce heat loss from the flat heating element.

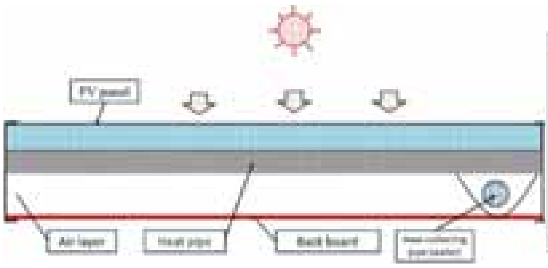


**Fig. 6: Schematic diagram of solar hybrid panel**

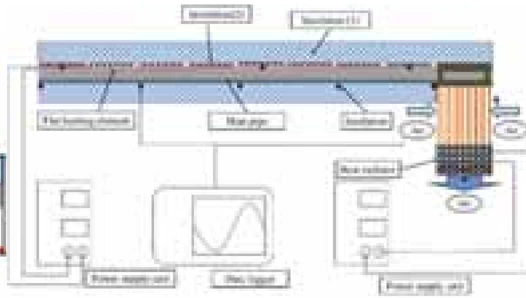

**Fig. 7: Diagram of experiment**

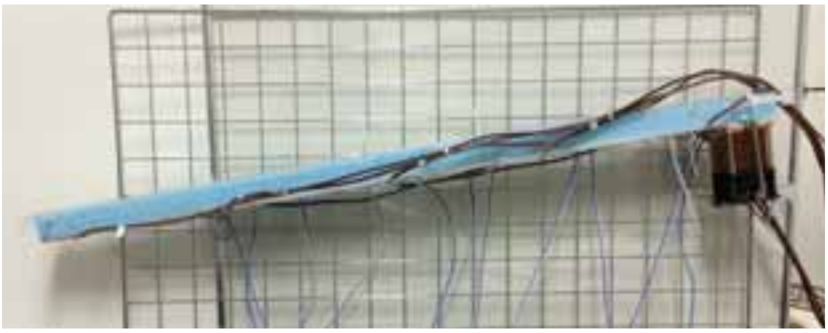

**Fig. 8: Experiment equipment**

### *5.2 Experiment cases*

There were five experiment parameters: angle of tilt, heat input, presence or lack of insulation on the back side, heat radiation air flow, and differences in length. The experiment was carried out for 64 cases by combining the parameters from Table 2. Measurement points are indicated in Table 3 and Fig. 9.

**Table 2: Experiment parameters**

| Parameter | Number of levels | Levels |
|---|---|---|
| Angle | 6 | 0°,5°,10°,20°,45°,90° |
| Heat input* | 5 | 217 W/m$^2$ (10 W) 435 W/m$^2$ (20 W) 651W/m$^2$ (30 W)<br>871 W/m$^2$ (40 W) 1085 W/m$^2$ (50 W) 1302W/m$^2$ (60 W) |
| Radiator air flow | 3 | Standard (0.033749 m$^3$/s) 50% 25% |
| Insulation | 2 | With insulation, without insulation |
| Heat pipe length | 2 | Type-M (60 mm × 765 mm), Type-L(60 mm × 955 mm) |

*Corresponds to intensity of solar radiation passing through PV panel.

**Table 3: Measurement points**

| Measurement points | Nounber oh points |
|---|---|
| Panel back side temperature | CH1, CH3, CH5, CH7, CH9 |
| Flat heating element | CH15,CH17,CH19 |
| Outside air temperature | CH11 |
| Outlet temperature | CH19 |

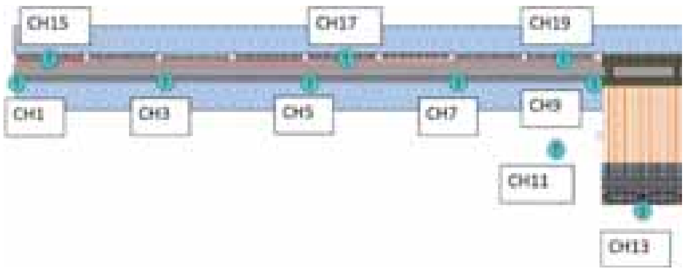


**Fig. 9: Measurement points**

### *5.3 Test results*

(1) Angle of tilt and heat input (Fig. 10)

As the angle of tilt of the heat pipe increases, the average back side temperature decreases, and the heat pipe functions normally. With low heat input of 10 W or 20 W, the back side average temperature decreases by 5 degrees or more. When heat input is 30 W or higher, the back side average temperature decreases with an angle of inclination of 10 degrees or more and there is also equalization of the temperature distribution. Therefore, it can be said that heat transport of the heat pipe functions properly if the angle of inclination is10 degrees or more.

(2) Heat radiation air flow (Fig. 11)

When heat radiation decreases, average temperature of the heat pipe back side rises. This is because a larger amount of heat is radiated when the air flow of the radiator is high. If heat input is high, the difference in temperature due to the difference in heat radiation increases. In the case with heat radiation air flow of 50% and heat input of 60 W, the back side average temperature rose by approximately 3ºC. The heat radiation performance is not affected very much with low heat input of around 10 W.

(3) Effects of insulation (Fig. 12)

In the case with insulation, back side average temperature is about 1°C higher than with no insulation. This is because, when there is no insulation, heat is radiated from the surface of the uninsulated heat pipe.

(4) Comparison of heat pipe length (Fig. 13)

A comparison was performed based on differences in length. When heat radiation air flow is low, the temperature of a long heat pipe rises somewhat, but otherwise there is hardly any difference.

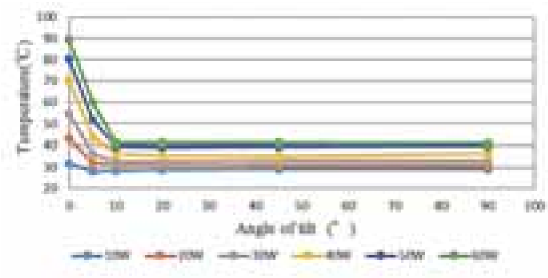

**Fig. 10: Relationship of angle of tilt and heat input different**

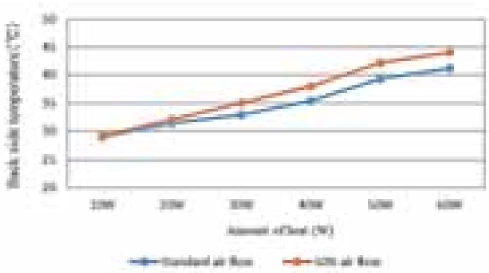

**Fig. 11: Comparison of back side temperatures with radiation air flow rates**

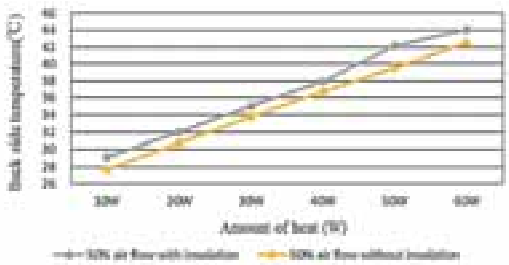

**Fig. 12: Comparison of back side temperatures with difference in insulation**

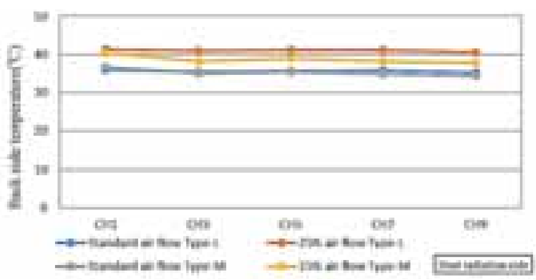

**Fig. 13: Results of length comparison corresponding to 40W to 40W**

## 6. Energy balance of the panel

A simulation model was created based on the schematic diagram (Fig. 14) of solar hybrid panel. The model was implemented in spreadsheet software using the heat balance equations given in Table 4. Table 6 shows the spreadsheet.

In the simulation, the heat-collecting pipe efficiency was defined by comprehensively taking into account factors such as the type of mounting of the heat-collection part and the water temperature. The PV panel was assumed to be integrated with glass (reflection and absorption only; thermal conductivity the same as glass), and surface reflectance was assumed to be 5%. The temperature difference at both sides of the heat pipe was assumed to be 1ºC. Thermal conductivity of the back side of the panel was assumed to be due to convection only and radiation was ignored because the surface is facing the rooftop. Thermal resistance of the acrylic panel on the back side was included in the thermal resistance of the air layer.

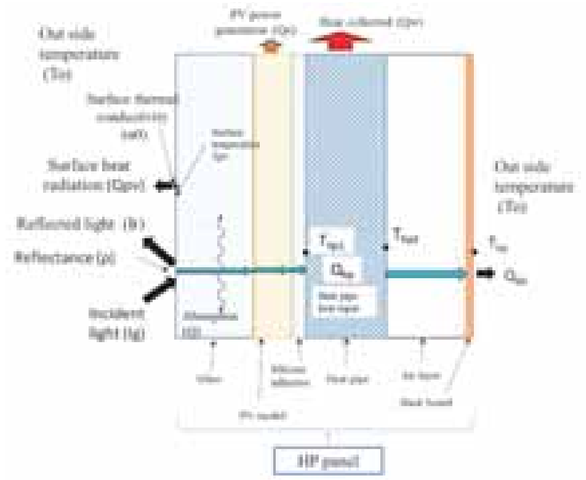


**Fig. 14 Energy balance schematic diagram**

**Table 4: Heat balance calculation equations**

| | | | | | |
|---|---|---|---|---|---|
| Amount of reflection | W/m² | Ir | = | (Ist+Isky)*ρ | (eq. 1) |
| Amount of heat absorption | W/m² | Ia | = | (1-ρ)*Is | (eq. 2) |
| PV panel surface temperature | ºC | Tpv | = | (Qw+Qbp)*R+Thp1 | (eq. 3) |
| Amount of heat radiation at PV surface | W/m² | Qpv | = | (Tpv-To)*αo | (eq. 4) |
| PV power generation | W/m² | Qe | = | Is*η | (eq. 5) |
| Thermal resistance | km2/W | R | = | Tpv/λpv+Tsi/λsi | (eq. 6) |
| HP surface temperature | ºC | Thp1 | = | Thp2+1.0 | (eq. 7) |
| HP heat input | W/m² | Qhp | = | Is-Ir-Qpv-Qe | (eq. 8) |
| Amount of heat collected | W/m² | Qw | = | Qhp*ηh | (eq. 9) |
| Heat collection efficiency | % | ηh | = | Qw/Is | (eq.10) |
| Heat balance | W/m² | Sh | = | Is-Ir-Qpv-Qw-Qbp-Qe | (eq. 11) |
| Precision | % | ε | = | Qw/Qwe | (eq. 12) |
| Surface heat transfer coefficient | W/m²K | αo | = | αor+αoc | (eq. 13) |
| Radiation | W/m²K | αor | = | ε0*4*σ*Tm^3 | (eq. 14) |
| | | | | ε0 assumes that radiation rate is 0.9 | |
| | | | | Tm=Tmp+273.16 | Tmp= Surface temperature of panel (assumed to be 40 ºC) |
| Convection | W/m²K | αoc | = | 5.0+3.4v (v≤5m/s) | (eq. 15) |
| | | | = | 6.14v^0.78(v>5m/s) | (eq. 16) |

**Table5: Symbols**

| Quantity | Symbol | Unit |
|---|---|---|
| Outside air temperature | *To* | ºC |
| PV panel surface temperature | *Tpv* | ºC |
| Heat pipe surface temperature | *Thp1* | ºC |
| HP back side temperature | *Thp2* | ºC |
| Back side temperature | *Tbp* | ºC |
| Intensity of solar radiation on tilted surface | *Is* | $W/m^2$ |
| Amount of reflection | *Ir* | $W/m^2$ |
| Amount of heat absorption | *Ia* | $W/m^2$ |
| Surface heat transfer coefficient | *αo* | $W/m^2K$ |
| Convection heat transfer coefficient | *αoc* | $W/m^2K$ |
| Radiation heat transfer coefficient | *aor* | $W/m^2K$ |
| Thermal conductivity | *αbp* | $W/m^2K$ |
| Thermal conductivity | *R* | $Km^2/W$ |
| Back side heat transfer coefficient | *Rair* | $Km^2/W$ |
| Amount of heat radiation at PV surface | *Qpv* | $W/m^2$ |
| PV power generation | *Qe* | $W/m^2$ |
| Heat pipe heat input | *Qhp* | $W/m^2$ |
| Amount of heat collected | *Qw* | $W/m^2$ |
| Amount of heat radiated at back side | *Qbp* | $W/m^2$ |
| Measured amount of heat collected | *Qwm* | $W/m^2$ |
| Heat balance | *Sh* | $W/m^2$ |
| PV power generation efficiency | $\eta$ | % |
| Heat pipe heat transfer efficiency | $\eta hp$ | % |
| Heat collection efficiency | $\eta h$ | % |
| Precision | $\varepsilon$ | % |
| Reflectance | $\rho$ | |
| Glass thickness | *tpv* | m |
| Silicone adhesive thickness | *tsi* | m |
| Wind speed | *v* | m/s |

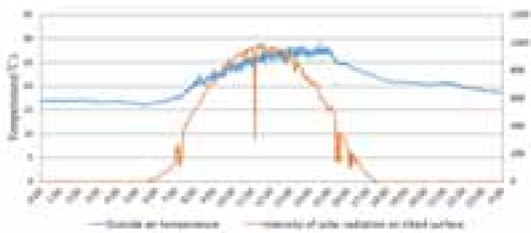

**Fig. 15: Outdoor air temperature and intensity of solar radiation on tilted surface (calculation)**

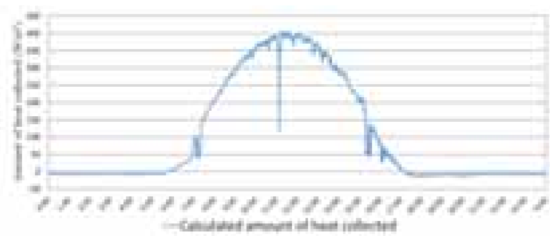

**Fig. 16: Amount of heat collection**

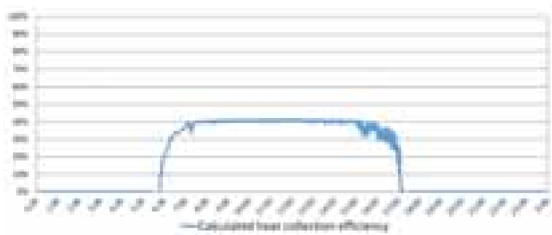

**Fig. 17: Heat collection efficiency (calculation)**

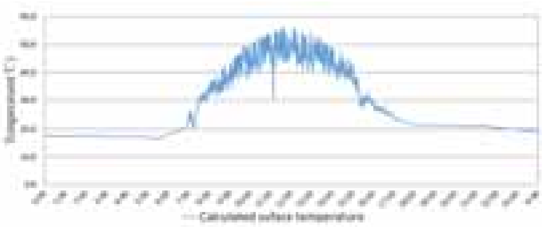

**Fig. 18: Heat pipe back side temperature (calculation)**

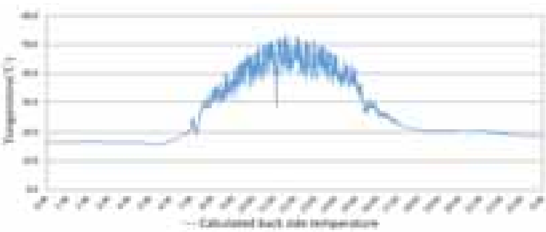

**Fig. 19: Heat pipe surface temperature (calculation)**

### *6.2 Energy balance sensitivity analysis*

Variation in the amount of heat collected was analyzed while varying the wind speed and silicone grease conductivity in the heat balance spreadsheet for the solar hybrid panel (Table 6). Fig. 20 and 21 graph the amount of heat collected when the wind speed and silicone grease conductivity are varied. The following points are evident in the results.

**Table 6: Heat balance spreadsheet for solar hybrid panel**

| Month | Day | Hour | Outside air temperature | Wind speed | Intensity of solar radiation on tilted surface | Reflectance | Amount of reflection | Amount of heat absorption | PV panel surface temperature | Surface heat transfer coefficient | Amount of heat radiation at PV surface | PV power generation efficiency | PV power generation | Glass thickness | Thermal conductivity |
|---|---|---|---|---|---|---|---|---|---|---|---|---|---|---|---|
| | | | To | v | Is | ρ | I r | Ia | Tpv | αo | Qpv | η | Qe | tpv | λpv |
| | | | ºC | m/s | W/m2 | - | W/m2 | W/m2 | ºC | W/m2K | W/m2 | % | W/m2 | m | W/mK |
| 9 | 22 | 11:30 | 25.3 | 0.7 | 972.8 | 0.05 | 48.6 | 924.2 | 48.1 | 13.65 | 311 | 0.12 | 116.7 | 0.002 | 0.78 |

| Silicone grease thickness | Thermal conductivity | Thermal resistance | Heat pipe surface temperature | Heat pipe heat input | Heat pipe heat transfer efficiency | Amount of heat collected | HP surface temperature | Thermal resistance of air layer | Back side temperature | Back side heat transfer coefficient | Amount of heat radiated at back side | Heat collection efficiency |
|---|---|---|---|---|---|---|---|---|---|---|---|---|
| tsi | λsi | R | Thp1 | Qhp | η | Qw | Thp2 | Rair | Tbp | αbp | Q b p | ηh |
| m | W/mK | Km2/W | ºC | W/m2 | % | W/m2 | ºC | Km2/W | ºC | W/m2K | W/m2 | % |
| 0.001 | 0.8 | 0.004 | 46.2 | 496.4 | 0.805 | 399.6 | 45.2 | 0.07 | 38.4 | 7.38 | 96.8 | 41% |

(1) Sensitivity analysis of thermal conductivity of the silicone adhesive.

Heat conduction performance of the silicone adhesive was evaluated. Thermal conductivity of the currently used silicon adhesive is 0.8 W/mK. If the silicon adhesive is changed to one with higher or lower thermal conductivity, there is almost no change in the amount of heat collected at and above 0.2 W/mK. This calculation is carried out assuming that thickness of the silicon adhesive is 1 mm, and therefore in the actual equipment the thickness is will be less, and the effect is likely to be even smaller.

(2) Sensitivity analysis of the wind speed

The amount of heat collected was compared when wind speed is varied. With a high wind speed, the convection heat efficiency increases, and thus the amount of heat collected decreases. It is evident that the size of this decrease is about 2%/(m/s).


**Fig. 20: Silicone adhesive conductivity sensitivity**

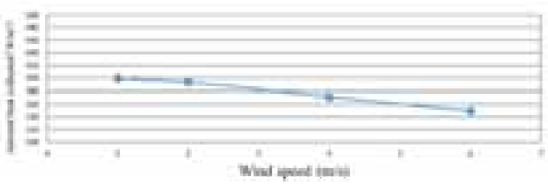


**Fig. 21: Wind speed sensitivity**

## 7. Conclusion

Basic experiments were carried out to develop an understanding of the characteristics of the heat pipe used in this solar hybrid panel. Also, a simulation model was created, and sensitivity was analyzed. The following findings were obtained as a result.

(1) Heat pipe properties

- Length of the heat pipe has little effect, and if the angle of tilt is at least 10 degrees, the system operates normally regardless of the intensity of solar radiation.

- If the heat radiation air flow rate is decreased, then temperature decreases when heat pipe temperature increases.

- When there is insulation, temperature of the heat pipe rises, and when there is no insulation, temperature of the heat pipe falls due to radiation of heat from the uninsulated surface.

(2) Energy balance simulation

- In sensitivity analysis of the energy balance, it was found that thermal conductivity of silicone adhesive does not have an effect on the amount of heat collected.

- In sensitivity analysis of wind speed, it was found that the amount of heat collected decreases as wind speed increases.

In the future, we plan to further evaluate performance of the solar hybrid system by measuring the amount of heat collected and the amount of power generated in the actual system.

## 8. References

Erkata Yandri, Naoto Hagino, Haruhiko Imada, Kazutaka Itako, Hiro Yoshida, Effect of internal heating on thermal performance of hybrid photovoltaic & thermal (PV/T) collector, 2011, SWC2011.